

Dedicated to my beloved parents,
Shri Binay Kumar Mishra (Papa)
Late Shrawan Kumar Pandey (Father-in-law)
and
Smt. Pushpa Mishra (Maa)
Smt. Durga Pandey (Mother-in-law)

for their blessings, endless support and
encouragement

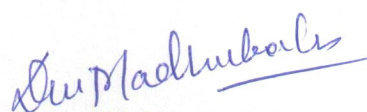
DECLARATION BY THE CANDIDATE

I hereby declare that the thesis "To study the snake venom nerve growth factor-derived custom peptides for their application in preventing Parkinson's disease" being submitted to Department of Molecular Biology and Biotechnology, Tezpur University, Tezpur, Assam in partial fulfillment for the award of the degree of Doctor of Philosophy in Molecular Biology and Biotechnology, has previously not formed the basis for the award of any degree, diploma, associateship, fellowship or any other similar title or recognition. Due to the unavailability of proper facilities at Tezpur University, the following experiments/sample analyses were carried out at other institutes:

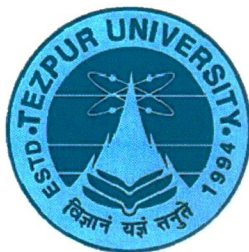
1. LC-MS/MS analysis of samples was performed at the Centre for Cellular and Molecular Platforms (C-CAMP) and Biokart, Bangalore, India. Transcriptomics and miRNA sequencing were performed at Biokart, Bangalore, India.
2. Confocal microscopic studies, Flow cytometry studies, and many other techniques were used at SAIC IASST, Guwahati 781035, India.
3. *In vitro* and *in vivo* experiments were performed at an animal experiment facility, IASST, Guwahati 781035, India.

Date:

Place: Tezpur


(Dev Madhubala)

Department of Molecular Biology and Biotechnology
School of Sciences, Tezpur University



TEZPUR UNIVERSITY

CERTIFICATE OF SUPERVISOR

This is to certify that the thesis entitled “**To study the snake venom nerve growth factor-derived custom peptides for their application in preventing Parkinson’s disease**” submitted to the School of Sciences, Tezpur University in requirement of partial fulfillment for the award of the degree of Doctor of Philosophy in Molecular Biology and Biotechnology is a record of research work carried out by Ms. Dev Madhubala under my supervision and guidance. All help received by her from various sources has been duly acknowledged. No part of this thesis has been submitted elsewhere for award of any other degree.

(Dr. A. K. Mukherjee, Ph.D., D.Sc., FASc., FRSB)

Designation: Professor

School: School of Sciences

Department: Molecular Biology and Biotechnology, Tezpur University (on deputation at IASST, Guwahati)

Present address: Director, Institute of Advanced Study in Science and Technology (IASST), Guwahati

Date: 14/10/2024

Place: Tezpur

ACKNOWLEDGEMENTS

First and foremost, I bow in front of the Almighty and thank Him for giving me the strength to make a humble contribution to society through my research work.

I express my respectful gratitude to my Ph.D. Supervisor, Prof. Ashis Kumar Mukherjee, thank you for introducing me to the exciting field of therapeutic application of snake venom. His relentless encouragement, insightful advice, and unrivaled support and guidance throughout my Ph.D. tenure enabled me to complete my research work. I deeply respect his dynamic vision, sincerity, and devotion toward research, and it was a great privilege and honor to work under his guidance.

I thank Prof V. K Jain and Prof. Shambhu Nath Singh, the former and present vice-chancellors of Tezpur University, respectively, for allowing me to work at this esteemed University. I have always felt fortunate to be a part of this University, which has a perfect environment for research among the students.

I am incredibly grateful to the Director, IASST, Guwahati, Dr. Mojibur R. Khan, and Dr. Jagat. C. Borah, Mr. Kangkan Saikia (Bioinformatics hub, IASST), faculty members, and staff of IASST Guwahati for providing me with laboratory facilities including lodging facility, and helping me conduct a major part of my research work at IASST.

I sincerely acknowledge the Heads of the Department of Molecular Biology and Biotechnology and Tezpur University for providing all possible facilities for my research work. I am also thankful to my Doctoral Committee members- Prof Manabendra Mandal, Dr. Venkata Satish Kumar Mattaparthi, Dr. Suman Dasgupta, Department of MBBT; all the members of the Departmental Research Committee and all the faculty members of the Department of MBBT for their valuable suggestions and inspiration throughout this study.

I also take this opportunity to thank Dr. K. K. Hazarika, Dr. N. K. Bordoloi, Mr. P. Mudoi, Mrs. Pranita S. Talukdar, Mr. Bijoy Mech, Mr. Guna Das, and all the non-teaching staff for all the help they have provided me during my Ph.D. tenure.

I also convey my thanks to Dr. Rupak Mukopadhyay, Dept. of MBBT, Tezpur University, for the in vitro study, Dr. Kavita Babu, Associate Professor IISc, Bangalore, for providing CAM-1(ak37) mutant strain, and Dr. Pedro Alexandrino Fernandes from Universidade do Porto, Portugal for guiding me with in silico studies.

I sincerely thank my lab seniors (Dr. Taufikul Islam, Dr. Debananda Gogoi, Dr. Bhargab Kalita, Dr. Sumita Dutta, and Dr. Abhishek Chanda) for their guidance. A special thanks to Dr. Aparup Patra for his constant guidance and help in every research step during my Ph.D. work. My lab mates (Nitisha, Bhabana, Upasana, and Hirak), and lab juniors (Anushree, Paran, Himangshu, Rozy, Rahul, and Bhagyalaksmi) for helped me in times I needed them most. I have enjoyed the research atmosphere of my lab and the unconditional support and love extended by my lab colleagues. I acknowledge Dr. Chandana Malakar, Dr. Arun Kumar, and Semim Ahmed from IASST for helping me with my experiments.


I also take this opportunity to thank all my seniors and friends from Tezpur University and IASST, Guwahati, whose company I enjoyed during my stay.

I sincerely thank DST-SERB, New Delhi, and Tezpur University (Institutional fellowship) for providing me with the company to conduct my research.

Last but not least, I thank my husband (Ashish Pandey), brothers (Krishna, Utsav, Arnab), and family members for their endless support and encouragement. Finally, I would like to thank all the people whose direct and indirect support helped me complete my research in time.

Place: Tezpur

Date:


(Dev Madhubala)

Contents	TABLE OF CONTENTS	Page no.
CHAPTER III		
MATERIALS AND METHODS		57-86
3.1 Materials		57
3.1.1 Synthetic custom peptides		57
3.1.2 Cell lines, cell culture reagents, and cell culture plastic wares		57
3.1.3 <i>Caenorhabditis elegans</i> strains and <i>Escherichia coli</i>		57
3.1.4 Neurotrophic factors and fine chemicals		57
3.2 Methods		58-82
3.2.1 To study the interaction of synthetic Custom Peptides with mammalian TrkA receptor and TrkA homolog in <i>C. elegans</i> by computational (<i>in silico</i>) analysis		58-60
3.2.1.1 Predicting the binding affinity of synthetic peptides to different domains of human TrkA receptors by <i>in silico</i> analysis		58-59
3.2.1.2 Predicting the binding affinity of synthetic peptides to different receptors in <i>C. elegans</i> by <i>in silico</i> analysis		59-60
3.2.2 To study the <i>in vitro</i> mechanism of neuritogenesis and neuroprotective role, of CPs in pheochromocytoma of the rat adrenal medulla (PC-12) cells		60-70
3.2.2.1 Solid-phase synthesis and biophysical characterization of the custom peptides		60
3.2.2.2 Cell growth and maintenance		
3.2.2.3 Assessing the binding of FITC-conjugated custom peptides to TrkA receptor-expressing mammalian cells		61-62
3.2.2.4 Assessing the <i>in vitro</i> cell cytotoxicity of the custom peptides		
3.2.2.5 <i>In vitro</i> effect of custom peptides on the mammalian hematological system		62
3.2.2.6 Assessing the neuritogenesis properties of custom peptides in PC-12 cells and the effects of chemical inhibitors on their neuritogenesis potency		62-63
3.2.2.7 Assessing the protective role of custom peptides against the PT-induced cytotoxicity in PC-12 cells		63-64
3.2.2.8 Flow cytometry analysis to determine PT-induced apoptotic cell death and its protection by custom peptides		64-65
3.2.2.9 Determination of the effect of custom peptides in inhibiting the reactive oxygen species (ROS) production in PT-treated PC-12 cells by spectrofluorometric assay and flow cytometry analysis		65-66

3.2.2.10 Determination of the effect of custom peptides on reducing the PT-induced depolarization of mitochondrial membrane potential	66
3.2.2.11 Determination of the effect of custom peptides on the restoration of PT-induced cellular and nuclear morphological changes in PC-12 cells	67
3.2.2.12 DPPH free radical scavenging activity of custom peptides <i>in vitro</i> condition	67
3.2.2.13 Quantitative reverse transcription-polymerase chain reaction (qRT-PCR) analysis to determine the expression levels of pro- and anti-apoptotic genes in the PT-treated PC-12 cells and the effect of pre-treatment of custom peptides	68-69
3.2.2.14 Quantitative proteomic analysis comparing the expression of global proteins for PC-12 cells exposed to PT and cells pre-treated with custom peptides followed by the PT treatment	69-70
3.2.3 To study the <i>in vivo</i> neuroprotective mechanism of CPs in <i>C. elegans</i>	
3.2.3.1 Maintenance of <i>C. elegans</i> strain	70-80
3.2.3.2 Determination of <i>in vivo</i> binding of FITC-conjugated custom peptides to <i>C. elegans</i> (CAM-1 mutant and N2 strains)	70-71
3.2.3.3 Assessment of the protective role of custom peptides against PT-induced toxicity in <i>C. elegans</i> (N2 and CAM-1 mutant strain)	71-72
3.2.3.4 PT-induced loss of chemotaxis behavior in <i>C. elegans</i> and its restoration by treatment with custom peptides	72
3.2.3.5 Determination of the effect of custom peptides in inhibiting the ROS production in PT-treated <i>C. elegans</i>	73-74
3.2.3.6 Determination of the effect of custom peptides on reducing the PT-induced depolarization of mitochondrial membrane potential	74-75
3.2.3.7 Quantitative analysis of the effect of custom peptides on PT-induced dopaminergic (DAergic) neurodegeneration	75
3.2.3.8 Quantitative analysis of the effect of custom peptides on preventing the α -synuclein accumulation in the NL5901 strain of <i>C. elegans</i>	75-76
3.2.3.9 Quantitative reverse transcription-polymerase chain reaction (qRT-PCR) analysis to determine the effect of pre-treatment of <i>C. elegans</i> with custom peptides on the PT-induced stress-related gene expression	76
3.2.3.10 Transcriptomic analysis to study the gene expression in <i>C. elegans</i> when treated with PT vs. pre-treatment with	76-78
	78-79

custom peptides followed by treatment with PT	
3.2.3.11 Quantitative proteomics analysis to compare the expression of global proteins between <i>C. elegans</i> pre-treated with custom peptides followed by PT and <i>C. elegans</i> treated only with PT	79-80
3.2.4 Study the micro-RNA expression profile in mouse 2.5 S-NGF and custom peptides-treated <i>C. elegans</i>	
3.2.4.1 Sequencing of miRNA to study the global miRNA expression profile and comparison between the PT group and PHNP group of <i>C. elegans</i>	80-82
3.2.4.2 Determination of acute <i>in vivo</i> toxicity and biochemical changes post-treatment of the peptides in a Swiss albino mice model	80-81
	81-82
3.2.5 Statistical analysis	82
Bibliography	82-86

Contents	TABLE OF CONTENTS	Page no.
CHAPTER IV		
Neurotrophic potency and mechanism of neuroprotective action of snake venom-derived custom peptides in pheochromocytoma of the rat adrenal medulla (PC-12) cells		87-134
4.1. Results		103-122
4.1.1 The biophysical characterization to ascertain the purity of the synthesized peptides		88-89
4.1.2 Computation analysis to predict the interaction between different domains of TrKA receptor and SV NGF-derived custom peptides		90-93
4.1.3 The FITC-conjugated custom peptides showed exclusive binding to mammalian cells expressing the TrkA receptor but not to cells with TrkB or TrkC receptors		93-95
4.1.4 Custom peptide-induced neurite outgrowth and differentiation of PC-12 cells		95-98
4.1.5 Chemical inhibition of TrkA receptor (K252a), PI3K/AKT (LY294002), and MAPK/ERK (U0126) pathways inhibited neuritogenesis induced by the custom peptides in PC-12 cells		98-99
4.1.6 Pre-treatment of PC-12 cells with custom peptides enhanced their cell survival against PT-induced cell death		100-102
4.1.7 Inhibition of PT-induced ROS production in PC-12 cells		103-105
4.1.8 Inhibition of PT-induced depolarization of mitochondrial		

membrane in PC-12 cells	105-107
4.1.9 Restoration of PT-induced cellular and nuclear morphological changes and apoptotic cells by the custom peptide pre-treated PC-12 cells	107-109
4.1.10 Custom peptide pre-treatment restored the paraquat-induced upregulated and downregulated pro- and anti- apoptotic genes to delay paraquat-induced programmed cell death in PC-12 cells	110
4.1.11 Comparing the differential expression of cellular proteins in the PT-treated PC-12 cells and the cells pre-treated with custom peptides by quantitative mass spectrometry	111-123
4.2. Discussion	123-129
Bibliography	129-134

TABLE OF CONTENTS

Contents	Page No.
CHAPTER V	
The <i>in vivo</i> neuroprotective mechanism of custom peptides in <i>Caenorhabditis elegans</i>	135-180
5.1 Results	135
5.1.1 <i>In silico</i> analysis of custom peptides binding in <i>C. elegans</i>	136-137
5.1.2 The confocal microscopic study shows <i>in vivo</i> binding of FITC-conjugated custom peptides to the nerve ring region of <i>C. elegans</i> N2 strain; however, an insignificant binding was observed with CAM-1 mutant strain of <i>C. elegans</i>	137-141
5.1.3 Pre-treatment with custom peptides reduced PT-induced worms' death and restored their chemotaxis dysfunction	141-144
5.1.4 Custom peptides inhibit PT-induced reactive oxygen species (ROS) production and depolarization of mitochondrial membrane potential in <i>C. elegans</i> N2 strain but could not protect CAM-1 mutant strain	144-149
5.1.5 Custom peptides restored PT-induced dopaminergic (DAergic) neurodegeneration and reduced α -synuclein accumulation in <i>C. elegans</i>	150-152
5.1.6 The custom peptides pre-treatment restores the PT-induced upregulated antioxidant/heat shock response/ p38 mitogen-activated protein kinase (MAPK) genes and delayed PT-induced programmed cell death in <i>C. elegans</i>	153-154
5.1.7 Transcriptomic analysis shows the differential expression of mRNA between PT-treated <i>C. elegans</i> and pre-treatment of <i>C. elegans</i> with custom peptides followed by PT-treatment	154-157
5.1.8 Quantitative proteomic analysis demonstrated differential	157-162

expression of cellular proteins between PT-treated and HNP peptide pre-treated followed by PT-treated <i>C. elegans</i>	
5.1.9 Transcriptomic and functional proteomics analyses in unison have elucidated the reversal of PT-induced upregulated and downregulated metabolic pathway genes by pre-treatment of <i>C. elegans</i> with neuroprotective peptide	163-166
5.1.10 The molecular network analysis demonstrates the neuroprotective functions of HNP against PT-induced toxicity and neuronal damage	167
5.1.11 Custom peptides were non-toxic to mice and safe to administer	168-170
5.2 Discussion	170-175
Bibliography	176-180

TABLE OF CONTENTS

Contents	Page No.
CHAPTER VI	
To study the microRNA expression profile in custom peptides-treated cultured <i>C. elegans</i>	181-198
6.1 Results	
6.1.1 Identification of mouse 2.5 S-NGF/custom peptide (HNP)-regulated miRNAs in <i>C. elegans</i> by miRNA sequencing analysis	182-187
6.1.2 A comparison of the differential expression of global miRNA between paraquat-treated <i>C. elegans</i> and pre-treatment of <i>C. elegans</i> with mouse 2.5 S-NGF/ HNP followed by paraquat treatment	187-192
6.2 Discussion	193-195
Bibliography	195-198
Chapter VII	
CONCLUSIONS AND FUTURE PERSPECTIVES	199-202
7.1 Conclusions	200
7.2 Future perspectives	201
7.3 Limitations of the study	202
Publications, Patents, and Conferences/Seminars	203-205
Appendix	206-223

LIST OF TABLES

Table No.	Table Captions	Page No.
CHAPTER-II		
2.1	Peptidomimetic-based treatment of NDs with neurotrophin.	41
CHAPTER-III		
3.1	List of oligonucleotide primer sequences for the quantitative reverse transcription-polymerase chain reaction (qRT-PCR) analysis in PC-12 cells.	69
3.2	List of oligonucleotide primer sets used for qRT-PCR analysis in <i>C. elegans</i> .	77-78
CHAPTER-IV		
4.1	The custom peptide sequences and their properties	91
4.2	Glide scores and molecular mechanics/generalized Born surface area (MM/GBSA) binding energy of custom peptides with domain 3 of human TrkA.	91
4.3	<i>In vitro</i> effect of custom peptides on mammalian blood.	96
4.4	The quantitative proteomics data shows the relative abundance of the intracellular proteins in the different treatment groups. The relative abundance of the proteins was calculated by the MS2-based spectral count method. For comparison of differential expression of the cellular proteins, the PC-12 cells were subjected to the following treatments at 37°C: (a) 1X PBS (control) treated PC-12 cells (CT), (b) 10 mM paraquat (PT) treatment for 24 h, (c) pre-treatment with 100 ng/mL (~71 nM) custom peptide for 1 h followed by 10 mM paraquat treatment (PHNP) for 24 h, and (d) treatment with 100 ng/mL (~71 nM) of custom peptide (HNP) for 1 h.	112-114
4.5	Comparison of the fold changes in differential expression of proteins in PT-treated PC-12 cells determined by proteomic analysis.	117-120
4.6	List of the uniquely expressed metabolic pathways in PC-12 cells treated with HNP when compared to untreated PC-12 cells. These pathways are determined by quantitative proteomic analyses.	121
CHAPTER-V		
5.1	List of the uniquely expressed metabolic pathways in <i>C. elegans</i> (N2) treated with HNP compared to untreated (control) <i>C. elegans</i> . Quantitative proteomic analyses determined these pathways.	160-162
5.2 A	(A) Transcriptomic and proteomic analyses to show the paraquat-induced upregulated metabolic pathways in wild-type N2 strain of <i>C. elegans</i> . These pathways were restored to control (normal) level by pre-treatment of worms with neuroprotective custom	162

	peptide HNP.	
5.2 B	(B) Transcriptomic and proteomics analyses to show the paraquat-induced downregulated metabolic pathways in N2 strain <i>C. elegans</i> . These pathways were restored to normal (control) levels by pre-treatment of worms with neuroprotective custom peptide HNP.	164-166
5.3	Some biochemical properties of serum of control and custom peptides (TNP and HNP; 1:1)-treated (10 mg/kg) mice after 24 hours of <i>i.v.</i> injection. Values are mean \pm SD of 6 mice. There was no significant difference in values ($p \geq 0.05$) between control and custom peptides-treated groups of mice.	169
Table no.	CHAPTER-VI	Page no
6.1A	(A) The miRNA microarray analysis data shows the fold changes of differentially regulated miRNA in the <i>C. elegans</i> treated with 50 μ g/mL of mouse 2.5 S-NGF (NGF) for 2 h with respect to 1X PBS-treated <i>C. elegans</i> (CT) at 20°C.	182
6.1B	(B) The miRNA microarray analysis data shows the fold changes of differentially regulated miRNA in the <i>C. elegans</i> treated with 50 μ g/mL of custom peptide (HNP) for 2 h compared to 1X PBS-treated <i>C. elegans</i> (CT) at 20°C.	183
6.1C	(C) Pathways annotation of potential miRNA target genes in only HNP/mouse 2.5 S-NGF-treated <i>C. elegans</i> .	183-185
6.2A	(A) The miRNA sequencing analysis data compares the fold changes in the differential expression of miRNA in the different treatment groups. Determination of toxicity of ASA, AAA and Ascorbic acid in <i>C. elegans</i> . Data represent mean \pm SD of three determinations.	189
6.2B	(B) The miRNA sequencing analysis data compares the fold changes in the differential expression of miRNA in the different treatment groups. For comparison of differential expression of the miRNA, the <i>C. elegans</i> were subjected to the following treatments at 20°C: (a) 1X PBS (control) treated <i>C. elegans</i> (CT), (b) 10 mM paraquat (PT) treatment for 1 h, (c) pre-treatment with 50 μ g/mL custom peptide for 2 h followed by 10 mM paraquat treatment (PHNP) for 1 h.	189-190
Table No.	Appendix Captions	Page No.
A1	Comparison of the fold changes in differential expression of proteins in paraquat-treated <i>C. elegans</i> determined by proteomic analysis.	205-208
A2	Predicted downstream targets of miRNA in PNGF and PHNP group of <i>C. elegans</i> .	209-221

LIST OF FIGURES

Figure Captions		
Figure No.	CHAPTER-I	Page No.
1.1	Age-standardized DALY rates of neurological disorders for both sexes and all ages among 204 countries and territories. (A) in 2019; (B) in 1990. This figure is adapted from [11].	3
1.2	Several mechanisms are allied with neurodegeneration that are concerned with the progression and pathogenesis of neurodegenerative diseases. This figure is adapted from [13].	4
1.3	Schematic presentation of the neurodegenerative disorder hallmarks and their subcellular location. Created with BioRender.com.	4
1.4	The pathophysiology of four major NDs - AD, PD, HD, and ALS. Created with BioRender.com.	7
1.5	The potential cytochrome c (a marker of apoptosis) is a danger-associated molecular pattern (DAMP). This figure is adapted from [40].	10
1.6	Protein family composition of western India (WI) Russell's viper venom (RVV). Nerve growth factor (NGF) constituting 4.8% of WI RVV proteome identified by tandem mass spectrometry analysis. This figure is adapted from [67].	12
1.6	Kegg pathway. Human neurotrophin signaling pathways.	14
Figure No.	CHAPTER-II	Page No.
2.1	Limitations associated with the clinical application and delivery of neurotrophic factors. Created with BioRender.com.	34
2.2	Trends in peptide therapeutic development. Created with BioRender.com.	36
Figure No.	CHAPTER-III	Page No.
3.1	The schematic diagram represents the experimental design of the chemotaxis assay to calculate the chemotaxis index (CI).	74
Figure No.	CHAPTER-IV	Page No.
4.1	HPLC chromatogram of the custom peptide (A) TNP, (B) HNP. MS/MS spectrum of the peptide (C) TNP, and (D) HNP was analyzed by ESI LC/MS-MS.	88-89
4.2	Circular dichroism (CD) spectra of custom peptides (A) TNP and (B) HNP. Custom peptides (0.3 mg/ml) were dissolved in 20 mM potassium phosphate buffer pH 7.0 and the far UV-CD spectra were recorded at room temperature (~25 °C) between 190 and 250 nm against the appropriate buffer (blank).	90
4.3	The <i>in silico</i> analysis of (A) Human TrkA receptor Chain A and B in complex with human NGF homodimer (PDB ID- 2IFG). The 3D	90

	model shows the interaction of TrkA with (B) TNP, and (C) HNP to form a ligand-receptor complex. The ball and stick structure represent peptide structure, and the string model corresponds to TrkA receptor domain-3.	
4.4	Molecular dynamic simulation of domain-3 backbone and custom peptides (A) TNP, (B) HNP shown in an RMSD (root mean square deviation) plot throughout the simulation trajectory for 300 ns.	92
4.5	Schematic diagram depicting the interaction of custom peptides (A) TNP (B) HNP with domain-3 of the TrkA receptor. The percentage of interaction is shown in the figure recorded over the simulation time of 300ns.	93
4.6	Fluorescence analysis to determine the (A) time-dependent binding (30 min to 360 min) of custom peptides (100 ng/mL, ~71nM) with the TrkA receptor of cells. L6 cells (non-TrkA expressing cells) were taken as control. Significance of difference in the binding of TNP (for 120 min to 360 min) with respect to HNP for MDA-MB-231, *p < 0.05. Significance of difference in the binding of TNP (for 30 min to 360 min) with respect to HNP for MCF7 and PC-12 cell line, #p < 0.05. (B) Binding of custom peptides with cell surface TrkA receptor of PC-12 cells in an increasing concentration of custom peptides (50 ng/mL to 1000 ng/ml, equivalent to 40 to 800 nM). Significance of difference in the binding between different concentrations for TNP *p < 0.05 and for HNP #p < 0.05. Significance of difference in the binding of TNP with respect to HNP, ^p < 0.05. (C) A hyperbola curve was plotted for change in λ_{max} ($\Delta\lambda_{max}$) against the concentrations (nM) of the custom peptide with TrkA receptor expressing PC-12 cells (1×10^4 cells) and the Kd value was determined using GraphPad Prism 8.1.1 software. The binding of FITC-custom peptide (100 ng/mL) with (D) MCF7, (E) MDA-MB-231, and (F) L6 cells was observed under fluorescence. The binding of custom peptides was also shown in the presence or absence of a chemical inhibitor of the Trk family (K252a). Magnification was 40X. Values are mean \pm SD of triplicate determinations.	94-95
4.7	Concentration-dependent <i>in vitro</i> cytotoxicity of synthetic peptides (TNP and HNP) and PT (10 mM, positive control) against mammalian cells. The cells were incubated with progressive concentrations of custom peptides (500 ng/mL to 2 μ g/mL) with mammalian cells (MCF7, PC-12, and L6 cells) at 37°C in a CO ₂ incubator for 24h. Determination of cytotoxicity by (A) MTT assay, and (B) LDH release assay. Significance of difference in the cell viability by MTT assay for paraquat-treated cells with respected TNP and HNP treated cells, *p < 0.05. Significance of difference in	96

	the cell viability by LDH release assay for Triton-X treated cells with respect to TNP and HNP treated cells, [#] p < 0.05. Values are mean ± SD of triplicate determinations.	
4.8	Concentration-dependent (12.5 to 100 ng/mL) determination of neurite outgrowth in rat pheochromocytoma (PC-12) cells treated with custom peptides (TNP & HNP) post 14 days of incubation at 37°C, 5% CO ₂ . The cells were observed under a phase-contrast microscope at 20x magnification. The appearance of neurite outgrowth from PC-12 cells is indicated by black arrows. (A) 1X PBS (control) treated cells, (B) mouse 2.5S-NGF treated cells, (C-E) TNP-treated cells with different concentrations (12.5 to 100 ng/mL), (F-H) HNP-treated cells with different concentrations (12.5 to 100 ng/mL). (I) Box and whisker plots represent average neurite outgrowth per cell (in μm). (J) Bar graph showing the percentage of differentiated cells (total number of cells showing neurite outgrowth) in custom peptide and mouse 2.5 S-NGF-treated PC-12 cells. The neurite length was determined using MOTIC IMAGE PLUS 3.0 software. Significance of difference in the controls with respect to mouse 2.5S-NGF, *p < 0.05. Significance of difference in mouse 2.5S-NGF with respect to TNP and HNP (at the concentration 100 ng/mL), [#] p < 0.05. Significance of difference in different concentrations for TNP, [^] p < 0.05 and for HNP, [¥] p < 0.05. Values are mean ± SD of triplicate determinations.	98
4.9	(A) Effect of small synthetic inhibitors of major signaling pathways on neuritogenesis potency of custom peptides (TNP, and HNP, 100 ng/mL equivalent to 71nM), and NGF (positive control, 100 ng/mL) in PC-12 cells. Significance of difference in the percent differentiation of control cells compared to NGF, TNP, and HNP when no inhibitor was added, [#] p ≤ 0.05. Significance of difference in the percent cell differentiation between with inhibitors (K-252a, U0126, and LY294002) and without inhibitors, [#] p ≤ 0.05 (B) Effect of anti-TrkA, TrkB, TrkC antibody (1:1000) on neuritogenesis potency of custom peptides (TNP, and HNP, 100 ng/mL equivalent to 71nM), and NGF (positive control) in PC-12 cells. Significance of difference in the percent cell differentiation between with anti-TrkA antibody and without inhibitors, *p ≤ 0.05. Values are mean ± SD of triplicate determinations.	99
4.10	Determination of the protective effects of custom peptides against PT-induced cell death. The viability of PC-12 cells was determined by MTT assay. (A) Pre-treatment of cells with custom peptides (100 ng/mL, ~71 nM) or vitamin C (10000 ng/mL) for 4 h followed by PT treatment for 24 h at 37°C in a CO ₂ incubator. *p ≤ 0.05, a significant difference between untreated (control) and PT-treated	100

cells; # $p \leq 0.05$, a significant difference between PT-treated cells with respect to mouse 2.5S-NGF and custom peptide pre-treated PC-12 cells. ^ $p \leq 0.05$, a significant difference of mouse 2.5S-NGF treated cells with respect to the peptide (TNP and HNP) treated cells. (B) Treatment of cells with PT for 24 h followed by treatment with custom peptide for 4h. There is no significant difference in the cell viability in PT-treated cells with respect to mouse 2.5S-NGF, Vit C, and peptide post-treatment. (C) The cells were simultaneously treated with custom peptides and PT for 24 h followed by an assay of cell viability. There is no significant difference in the cell viability in PT-treated cells with respect to mouse 2.5S-NGF, Vit C, and peptide co-treatment. Values are mean \pm SD of triplicate determinations.

- 4.11 Determination of the optimum time and doses of peptide for neuroprotective activity against PT-induced toxicity. Time and dose-dependent neuroprotective activity was determined by MTT and LDH assay in PC-12 cells. (A) Pre-treatment of cells with custom peptides (100 ng/mL, ~ 71 nM) at a different time interval (0.5 h - 6 h) followed by PT treatment for 24 h at 37°C in a CO₂ incubator. * $p \leq 0.05$, a significant difference between untreated (control) and PT-treated cells; # $p \leq 0.05$, a significant difference of PT-treated cells with respect to custom peptide (TNP and HNP) pre-treated PC-12 cells for different time intervals (0.5 - 6 h). Significance of difference in the percent cell viability of custom peptide pre-treated cells incubated for 1 h with respect to 0.5-6 h, ^ $p \leq 0.05$. (B) Pre-treatment of cells with different concentrations of custom peptides (12.5 ng/mL to 500 ng/mL) for 1h (optimum time) followed by PT treatment for 24 h at 37°C in a CO₂ incubator (C) LDH release assay to determine the protective effects of custom peptides on the LDH release of PT-induced PC-12 cell cytotoxicity when pre-treated with different concentrations of custom peptides (25 ng/mL to 500 ng/mL) for 1h followed by PT treatment for 24 h at 37°C in a CO₂ incubator. * $p \leq 0.05$, a significant difference between untreated (control) and PT-treated cells; # $p \leq 0.05$, a significant difference of PT-treated cells with respect to custom peptide (TNP and HNP) pre-treated PC-12 cells for different time intervals (0.5-6 h). Significance of difference in the percent cell viability of custom peptide pre-treated cells at the dose of 100 ng/mL with respect to 12.5-500 ng/mL, ^ $p \leq 0.05$. Values are mean \pm SD of triplicate determinations. 101-102
- 4.12 Determination of PT-induced intracellular ROS generation and its reversal by pre-treatment with custom peptide (12.5 ng/mL to 500 ng/mL) and Vitamin C (positive control, 10000 ng/mL) for 1 h 103-104
-

followed by the PT treatment for 24 h at 37°C in a CO₂ incubator. The ROS generation was determined by using an H₂DCFDA fluorescence probe and expressed as a fold change value with respect to the control (1x PBS). (A) Determination of *in vitro* concentration-dependent (25-250 ng/mL) DPPH radical-scavenging activity of custom peptides. *p < 0.05 significant difference between different concentrations of custom peptide HNP; #p < 0.05 significant difference between the different concentrations of vit C. (B-D) Flow cytometric determination of intracellular ROS. (E) Bar graph representing quantitative analysis of the intracellular ROS generation (expressed by fold change value with respect to control) determined by flow cytometry analysis. *p ≤ 0.05, a significant difference between untreated (control) and PT-treated cells; #p ≤ 0.05, a significant difference of PT-treated cells with respect to custom peptides (TNP and HNP) and vit C pre-treated cells. Significance of difference in the fold change value in between TNP and HNP at the dose of 12.5 to 100 ng/mL, ^p ≤ 0.05. Values are mean ± SD of triplicate determinations.

- 4.13 Spectrofluorometric determination of intracellular ROS. *p < 0.05, a significant difference between untreated (control) and PT-treated cells; #p < 0.05, a significant difference of PT-treated cells with respect to custom peptides (TNP and HNP) and Vit C pre-treated cells. Significance of difference in the fold change value between TNP and HNP at the dose of 12.5 to 100 ng/mL, ^p < 0.05. Values are mean ± SD of triplicate determinations. 105
- 4.14 Reversal of PT-induced disruption of mitochondrial membrane potential (MMP) of PC-12 cells pre-treated with custom peptides (100 ng/mL, ~71 nM) for 1 h followed by the PT treatment for 24 h at 37°C in a CO₂ incubator. The PT-treated (10 mM) PC-12 cells pre-treated with or without custom peptide (~71 nM) were observed for the measurement of the ratio of red/green fluorescence intensity by JC-1 staining. (A) Confocal images of PC-12 cells stained with JC-1 dye to measure the MMP micrographed at the magnification of 40X. JC-1 red fluorescence represents normal MMP, whereas JC-1 green fluorescence indicates damaged MMP. The scale bar indicates the length as 20 μm. (B) Bar diagram representing the ratio of red/green fluorescence intensity quantified using Image J software. (C) The fluorescence signal intensity of JC-1 monomer and JC-1 aggregates was determined by flow cytometry analysis. Carbonyl cyanide m-chlorophenyl hydrazone (CCCP) is a mitochondrial uncoupling agent that depolarises the mitochondria taken as a positive control. (D) Bar graph representing quantitate analysis of the red and green fluorescence intensity detected by the flow 106-107
-

-
- cytometry. * $p \leq 0.05$, a significant difference between untreated (control) and PT-treated cells; # $p \leq 0.05$, a significant difference of PT-treated cells with respect to custom peptides (TNP and HNP) pre-treated cells. Significance of difference in fluorescence intensity between TNP and HNP, ^ $p \leq 0.05$. Values are mean \pm SD of triplicate determinations.
- 4.15 Effects of the custom peptide (100 ng/mL) on inhibition of PT-induced apoptosis in PC-12 cells pre-treated with custom peptides (100 ng/mL, ~71 nM) for 1 h followed by the PT treatment for 24 h at 37°C in a CO₂ incubator. (A) The fluorescence intensity of Annexin V-FITC and Propidium iodide (PI) was determined by flow cytometry. (B) The bar graph represents a quantitative analysis of the percent cell death determined by flow cytometry analysis. * $p \leq 0.05$, a significant difference between untreated (control) and PT-treated cells; # $p \leq 0.05$, a significant difference of PT-treated cells with respect to custom peptides (TNP and HNP) pre-treated cells. Significance of difference in percent cell death between TNP and HNP, ^ $p \leq 0.05$. Values are mean \pm SD of triplicate determinations. 108
- 4.16 Effects of the custom peptide (100 ng/mL) on inhibition of PT-induced apoptosis in PC-12 cells pre-treated with custom peptides (100 ng/mL, ~71 nM) for 1 h followed by the PT treatment for 24 h at 37°C in a CO₂ incubator. (A) Confocal microscopic analysis of changes in the cellular and nuclear morphology of PC-12 cells by DAPI staining at the magnification of 40X. The red arrows indicate cells with membrane blebbing and shrunken nuclei, and the white (solid) arrows indicate secondary cellular necrosis. The scale bar indicates the length of 20 μ m. (B) The bar diagram shows the percent cell death determined from the changes in the cellular and nuclear morphology with respect to the control (1x PBS). The intensity of the DAPI staining was determined using Image J software. * $p < 0.05$, a significant difference between untreated (control) and PT-treated cells; # $p < 0.05$, a significant difference of PT-treated cells with respect to custom peptides (TNP and HNP) pre-treated cells. Significance of difference in percent cell death between TNP and HNP, ^ $p < 0.05$. Values are mean \pm SD of triplicate determinations. 109
- 4.17 The qRT-PCR analysis to show the expression of key pro-/anti-apoptotic genes in PC-12 cells post-treatment with paraquat (10 mM) for 12 h, and comparison with the custom peptides (100 ng/mL, ~71 nM) /mouse 2.5S-NGF (positive control, 100 ng/mL) pre-treatment for 1 h followed by the PT treatment for 12 h at 37°C in a CO₂ incubator. The expression of mRNA was normalized using 110
-

	the housekeeping gene GAPDH. *p ≤ 0.05, a significant difference between untreated (control) and PT-treated cells; #p ≤ 0.05, a significant difference of PT-treated cells with respect to custom peptides (TNP and HNP)/mouse 2.5S-NGF pre-treated cells. Values are mean ± SD of triplicate determinations.	
4.18	(A) Venn diagram showing the common intracellular proteins among untreated (control) (CT), PT (PT) treated, and HNP pre-treated followed by PT-treated (PHNP) groups of PC-12 cells determined by LC/MS-MS analysis. (B) Venn diagram showing common intracellular proteins among untreated (control) (CT) and only HNP-treated PC-12 cells determined by LC/MS-MS analysis.	115
4.19	Molecular network of HNP-mediated neuroprotection drawn in Cytoscape (version 3.9.1). The molecular network shows the multiple pathways that are interconnected to each other and involved in the HNP-mediated neuroprotection. The proteins involved in the pathways were determined by LC/MS-MS analysis.	122
4.20	The proposed neuroprotection mechanism of custom peptides against PT-induced neurotoxicity in PC-12 cells.	123

Figure No.	CHAPTER-V	Page No.
5.1	Custom peptide interaction of TNP (left) and HNP (right) complex with (A) CED9, (B) PMK2, (C) CAM1-IG domain, and (D) CAM1-FZ domain shown in cartoon representation. Root mean square deviation (RMSD) plot of TNP (left) and HNP (right) complex with (E) CED9, (F) PMK2, (G) CAM1-IG domain, and (H) CAM1-FZ domain.	137
5.2	Confocal microscopic (40 X) studies of the <i>in vivo</i> binding of FITC-custom peptides to <i>C. elegans</i> for 2h. (A) Dose-dependent (12.5 µg/mL – 100 µg/mL) binding of custom peptides to the <i>C. elegans</i> . The scale bar indicates the length as 100 µm. (B) Bar graph representing fluorescence intensity between the treatment groups; *p < 0.05, a significant difference between 12.5 µg/mL and 25 µg/mL dose of FITC-conjugated peptides to <i>C. elegans</i> , #p < 0.05, a substantial difference between 25 µg/mL and 50 µg/mL dose of FITC-conjugated peptides to <i>C. elegans</i> . (C) Time-dependent (1 h – 4 h) binding of custom peptides (50 µg/mL) to the <i>C. elegans</i> . (D) Bar graph representing fluorescence intensity between the treatment groups (E) Microscopic image of the custom peptide binding to <i>C. elegans</i> in pre-treatment, post-treatment, and co-treatment conditions (with various concentrations of PT). The scale bar indicates the length as 100 µm. (F) Bar graph representing fluorescence intensity between the treatment groups; Significant difference between the pre-treatment, post-treatment, and co-treatment	138-140

-
- with FITC-custom peptide HNP compared to binding of only FITC-conjugated HNP to *C. elegans*, #p < 0.05.
- 5.3 (A) Confocal microscopic (40 X) studies of the *in vivo* binding of FITC-custom peptides (50 µg/mL, 2 h) to CAM-1 mutant and compared with wild-type N2 strain *C. elegans*. The scale bar indicates the length as 100 µm. (B) Bar graph representing fluorescence intensity between the CAM-1 mutant and N2 strains. *p < 0.05, a significant difference between CAM-1 mutant and N2 strain of *C. elegans*. Values are mean ± SD of triplicate determinations. 141
- 5.4 Determination of the effect of the custom peptide on PT-induced death of *C. elegans*. (A) worms were pre-incubated with mouse 2.5S-NGF (50 µg/mL)/quercetin (50 µg/mL, positive control) / vitamin C (100 µg/mL, positive control) and progressive concentration of custom peptides (12 µg/mL - 100 µg/mL) followed by the PT (10 mM) treatment. *p ≤ 0.05, a significant difference between untreated (control) and PT-treated cells; #p ≤ 0.05, a significant difference between PT-treated cells and quercetin/ mouse 2.5S-NGF/ vitamin C and custom peptide pre-treated *C. elegans*. ^p ≤ 0.05 Significance of difference in different concentrations for custom peptides. (B) worms were pre-incubated with quercetin (50 µg/mL, positive control) and custom peptides (50 µg/mL) for 2 h, 12 h, and 24 h followed by the PT (10 mM) treatment. *p ≤ 0.05, a significant difference between untreated (control) and PT-treated cells; #p ≤ 0.05, a significant difference between PT-treated cells and quercetin (positive control) and custom peptide pre-treated *C. elegans*. ^p ≤ 0.05, a significant difference between quercetin pre-treated *C. elegans* and the peptide (TNP and HNP) pre-treated *C. elegans*. (C) Worms were incubated with PT (10 mM) for 1 h and treated with custom peptides (12 µg/mL to 100 µg/mL). Freshly prepared custom peptides were added after 12 h of pre-incubation for 24 h pre-incubation condition. Worms were counted under a stereo zoom microscope for 30 s up to 24 h of treatments. Values are mean ± SD of triplicate determinations. (D) Determination of the effect of the custom peptides on PT-induced death of cam-1 mutant compared with wild type N2 strain of *C. elegans*. Worms were pre-incubated with custom peptides (50 µg/mL) followed by the PT (10 mM) treatment. Percent neutralization was calculated against only paraquat-treated worms. *p < 0.05, a significant difference between wild-type and cam-1 mutant strain. (E) Restoration of chemosensory behavior in *C. elegans* pre-treated with custom peptides. 143
-

Synchronized L4 stage *C. elegans* wide-type strain N2 was incubated with or without 50 µg/mL custom peptides. They were then subjected to PT-treatment (10 mM) and a chemosensory assay. * $p \leq 0.05$, a significant difference between untreated (control) and PT-treated cells; # $p \leq 0.05$, a significant difference between PT-treated cells and quercetin (positive control) and custom peptide pre-treated *C. elegans*. ^ $p \leq 0.05$, a significant difference between quercetin pre-treated *C. elegans* and the peptide (TNP and HNP) pre-treated *C. elegans*. Values are means \pm SD of triplicate determinations.

5.5 Determination of PT-induced intracellular ROS generation and its reversal by pre-treatment with custom peptide in wild type N2 strains of *C. elegans*. The ROS generation was determined by using an H₂DCFDA fluorescence probe. (A) spectrofluorometric determination of intracellular ROS. * $p < 0.05$, the significant difference between untreated (control) and PT-treated worms; # $p < 0.05$, the significant difference between PT-treated and custom peptide-treated worms. (B) confocal microscope images of nematodes expressing ROS. The scale bar indicates the length as 100 µm. (C) Bar graph representing dosimetry analysis of confocal images to quantitate the intracellular ROS generation. Error bars indicating SD (n=3). * $p < 0.05$, the significant difference between untreated (control) and PT-treated worms; # $p < 0.05$, the significant difference between PT-treated and custom peptide-treated worms. ^ $p \leq 0.05$, a significant difference between Vit C/ mouse 2.5 S-NGF pre-treated *C. elegans* and the peptides (TNP and HNP) pre-treated *C. elegans*. Values are means \pm SD of triplicate determinations. (D) confocal microscope images of nematodes expressing ROS. The scale bar indicates the length as 100 µm. (E) Bar graph representing dosimetry analysis of confocal images to quantify intracellular ROS generation. (F) Confocal images of *C. elegans* showing reversal of PT-induced disruption of mitochondrial membrane potential (MMP) of *C. elegans* pre-treated with custom peptides. The scale bar indicates the length as 100 µm. The scale bar indicates the size as 100 µm. The PT-treated (10 mM) N2 wild-type strain of nematodes pre-treated with or without custom peptide (50 µg/mL) was observed to measure the red/green fluorescence intensity ratio by JC-1 staining. (G) Bar diagram representing the red/green fluorescence intensity ratio quantified using Image J software. * $p \leq 0.05$, a significant difference between untreated (control) and PT-treated worms; # $p \leq 0.05$, a significant difference

146-149

between PT-treated and custom peptide pre-treated worms. $\hat{p} \leq 0.05$, a significant difference between the two peptides (TNP and HNP) pre-treated *C. elegans*. Values are means \pm SD of triplicate determinations. (H) Confocal images of CAM-1 mutant strain of *C. elegans* showing reversal of PT-induced disruption of mitochondrial membrane potential (MMP) of *C. elegans* pre-treated with custom peptides. The scale bar indicates the length as 100 μ m. The scale bar indicates the size as 100 μ m. The PT-treated (10 mM) N2 wild-type strain of nematodes pre-treated with or without custom peptide (50 μ g/mL) was observed to measure the red/green fluorescence intensity ratio by JC-1 staining. (I) Bar diagram representing the red/green fluorescence intensity ratio quantified using Image J software. $*p \leq 0.05$, a significant difference between untreated (control)/only custom peptide treated group and PT/custom peptide and PT-treated group of cam-1 mutant worms

- 5.6 Determination of dopaminergic neurodegeneration induced by PT in BZ555 *C. elegans*. (A) Confocal microscopic images (40 X) of DA neurons emerging GFP fluorescence signals in PT-treated BZ555 worms with or without pre-treated with custom peptides (50 μ g/mL). The scale bar indicates the length as 100 μ m. (B) The bar diagram shows the GFP fluorescence intensity indicating the content of DA neurons in BZ555 worms, quantified using the Image J software. $*p \leq 0.05$, a significant difference between untreated (control) and PT-treated worms; $\#p \leq 0.05$, a significant difference between PT-treated and custom peptide-treated worms. Custom peptides inhibit the aggregation of α -synuclein in transgenic NL5901 strains of *C. elegans*. (C) Confocal images of custom peptides (50 μ g/mL)-treated NL5901 worms after 12 h of incubation. The scale bar indicates the length as 100 μ m. (D) The bar chart shows the fluorescence intensity representing the α -synuclein protein accumulation in custom peptide-treated NL5901 worms for 12 h. $*$ ($p \leq 0.05$) a significant difference between control (CT) and custom peptides-treated *C. elegans*, $\#$ ($p \leq 0.05$) a significant difference between TNP and HNP treated *C. elegans*. Values are means \pm SD of triplicate determinations. 151-152
- 5.7 The qRT-PCR analysis shows the genes' expression in stress resistance, innate immunity, and apoptotic pathways in the PT-treated *C. elegans*, compared with the vitamin C (positive control)/custom peptide pre-treated *C. elegans*. The expression of mRNA was normalized using the housekeeping gene act-1. $*$ ($p \leq 0.05$) a significant difference between control (CT) and PT- 154

-
- treated *C. elegans*, # ($p \leq 0.05$) a significant difference between PT-treated and vitamin C/ custom peptide pre-treated worms. Values are means \pm SD of triplicate determinations.
- 5.8 Differential expression of genes between different treated groups of *C. elegans*. (A) PCA score plot showing the gene expression variability between the groups of *C. elegans* and within the biological replicates. (B) Correlation plot showing a correlation between treated groups of *C. elegans*. CT: untreated worms, PT: PT treated worms, PHNP: custom peptide HNP pre-treatment followed by PT treatment, HNP: custom peptide HNP treated worms. Plots showing differential expression of genes in PT-treated *C. elegans* and their restoration with peptide (HNP) pre-treatment. (C) Volcano plot (p-value v/s log Fc) for PT group versus CT group. (D) scatter plot displaying the statistically significant differentially altered genes between PT treatment and control group (PT vs. CT). (E) Volcano plot (p-value v/s log Fc) for PHNP group versus PT group (F) scatter plot displaying the statistically significant differentially altered genes between peptide HNP pre-treated *C. elegans* followed by PT treatment and PT-treated *C. elegans*. CT: untreated worms, PT: PT treated worms, PHNP: custom peptide HNP pre-treatment followed by PT treatment, HNP: custom peptide HNP treated worms. (G) Heat map showing the differential expression of the upregulated and downregulated genes among different groups of *C. elegans*. PT: PT treated, PHNP: peptide HNP pre-treatment followed by PT treatment, CT: untreated (control) worms. 155-157
- 5.9 Proteomics analysis to show the expression of common and intracellular proteins among the treated groups of *C. elegans*. (A) Venn diagram showing common intracellular proteins among untreated (control) (CT), PT (PT) treated, and HNP pre-treated followed by PT-treated (PHNP) groups of *C. elegans* determined by LC/MS-MS analysis. (B) Scatter plot showing significantly upregulated (fold change >1.25) and downregulated (fold change <0.80) proteins in PT-treated *C. elegans*. FC: fold-change in expression determined by LC/MS-MS analysis. (C) Venn diagram showing common intracellular proteins among untreated (control) (CT) and only HNP-treated *C. elegans* determined by LC/MS-MS analysis. (D) Molecular network of custom peptide HNP-mediated neuroprotection. The interaction network of peptide HNP-regulated genes/proteins and interlinking pathways as determined by both transcriptomic and proteomic analyses. 158-159
-

5.10	The proposed neuroprotection mechanism pathways of custom peptide mediated protection against PT-induced neurotoxicity in <i>C. elegans</i> (N2 strain).	167
5.11	The effect of the custom peptides (TNP: HNP:: 1:1) treatment on histological changes in the tissues of Swiss albino mice. The H and E staining was employed to observe any morphological changes in the tissues compared to those of the control (untreated). Light microscopic observation of (A) Brain, (B) Heart, (C) Kidney, (D) Liver, (E) Lung, (F) Ovary, and (G) Testis for control and treated groups. Bar-100µM.	169
5.12	Determination of the concentration of pro-inflammatory cytokines in control (1X PBS treated)/ custom peptides-treated (10 mg/kg) group of mice plasma by Quantikine HS ELISA Kit. * A significant difference between control (1X PBS-treated) and custom peptide (TNP:HNP)-treated <i>C. elegans</i> (p < 0.05). Values are means ± SD of triplicate determinations.	170

Figure no.	CHAPTER-VI	Page No.
6.1	Differential expression of miRNAs between mouse 2.5S-NGF/peptide HNP-treated group of <i>C. elegans</i> and 1X PBS-treated (control) group of <i>C. elegans</i> . (A) Volcano plot (p-value v/s log Fc) for mouse 2.5S-NGF-treated (NGF group) versus 1X PBS-treated (CT group) <i>C. elegans</i> . (B) Volcano plot (p-value v/s log Fc) for custom peptide HNP-treated (HNP group) versus 1X PBS-treated (CT) <i>C. elegans</i> . Heat map showing the differential expression of the upregulated and downregulated genes among (C) mouse 2.5S-NGF-treated (NGF group) versus 1X PBS-treated (CT group) <i>C. elegans</i> and (D) custom peptide HNP-treated (HNP group) versus 1X PBS-treated (CT) <i>C. elegans</i> .	186
6.2	Roles of mouse 2.5S-NGF and HNP-induced miRNAs involved in different stages of neuronal development in <i>C. elegans</i> .	187
6.3	Differential expression of miRNAs between different treated groups of <i>C. elegans</i> . (A-C) PCA score plot showing the gene expression variability between the groups of <i>C. elegans</i> and within the biological replicates. (D-F) Correlation plot showing a correlation between treated groups of <i>C. elegans</i> . (G) Volcano plot (p-value v/s log Fc) for PNGF group versus PT group and (H) Volcano plot (p-value v/s log Fc) for PHNP group versus PT group of <i>C. elegans</i> . CT: untreated worms, PT: PT treated worms, PHNP: custom peptide HNP pre-treatment followed by PT	188

	treatment, PNGF: mouse 2.5S-NGF pre-treatment followed by PT treatment HNP: custom peptide HNP treated worms, NGF: mouse 2.5S-NGF treated worms.	
6.4	Heat map showing the differential expression of the upregulated and downregulated miRNAs among different groups of <i>C. elegans</i> . (A) PNGF group versus PT group (B) PHNP group versus PT group of <i>C. elegans</i> . CT: untreated worms, PT: PT treated worms, PHNP: custom peptide HNP pre-treatment followed by PT treatment, PNGF: mouse 2.5S-NGF pre-treatment followed by PT treatment HNP: custom peptide HNP treated worms, NGF: mouse 2.5S-NGF treated worms.	191
6.5	Network of miRNA and their target genes for (A) PNGF and (B) PHNP group of <i>C. elegans</i> . The interaction network miRNA and their target genes were drawn by using Cytoscape 3.9.1.	192

ABBREVIATIONS

Abbreviation	Full form
AD	Alzheimer's Disease
ANOVA	One-Way Analysis of Variance
ATCC	American Type Culture Collection
ATP	Adenosine Triphosphate
BBB	Blood-Brain Barrier
BDNF	Brain-Derived Neurotrophic Factor
CD	Circular Dichroism
CID	Collision-Induced Dissociation
DAPI	4',6-Diamidino-2-Phenylindole
DMEM	Dulbecco's Modified Eagle Medium
DMSO	Dimethyl Sulfoxide
FBS	Fetal Bovine Serum
FITC	Fluorescein Isothiocyanate
HD	Huntington's Disease
HNP	Heptadeca-Neuropeptide
L6	Rat Myoblast or Myogenic Cells
LDH	Lactate Dehydrogenase
MAPK	Mitogen-Activated Protein Kinase
MDA-MB-231	Human Breast Adenocarcinoma Cells
MCF-7	Michigan Cancer Foundation-7
EMEM	Eagle's Minimum Essential Medium
ADP	Adenosine Diphosphate
AMP	Adenosine Monophosphate
ATP	Adenosine Triphosphate
CCCP	Carbonyl Cyanide M-Chlorophenylhydrazone
CGC	<i>Caenorhabditis</i> Genetics Center
CTAB	Cetyltrimethylammonium Bromide
DBP	Disulfide Bridge Peptide
DCF	2',7'-Dichlorodihydrofluorescein
DTT	Dithiothreitol
DPPH	2,2-Diphenyl-1-Picrylhydrazyl

Abbreviation	Full Form
FPLC	Fast Protein Liquid Chromatography
HCL	Hydrochloride
H ₂ DCFDA	2',7'-Dichlorofluorescein-Diacetate
HEPES	4-(2-Hydroxyethyl)-1-Piperazineethanesulfonic Acid
LC ₅₀	Median Lethal Concentration
LC/ES-MS	Liquid Chromatography-Electrospray Tandem Mass
LC-MS/MS	Spectrometry
LPP	Liquid Chromatography-Tandem Mass Spectrometry
LD ₅₀	Median Lethal Dose
MALDI-TOF-	Matrix-Assisted Laser Desorption/Ionization -Time Of Flight - Mass Spectrometry
NCBI	National Center For Biotechnology Information
NGM	Nematode Growth Media
MMGBSA	Molecular Mechanics/Generalized Born Surface Area
MMP	Mitochondrial Membrane Potential
MTT	3-(4,5-Dimethylthiazol-2-Yl)-2,5-Diphenyltetrazolium Bromide
NCBS	National Centre For Cell Science
NDs	Neurodegenerative Disorders
NGF	Nerve Growth Factor
P ⁷⁵ NTR	P75 Neurotrophin Receptor
PC-12	Adrenal Pheochromocytoma Cell Line
PD	Parkinson's Disease
PDB	Protein Data Bank
PI	Propidium Iodide
PI3K	Phosphatidylinositol 3-Kinase Stimulation Of Protein Kinase B Signaling Pathways
PPI	Protein-Protein Interaction
PPP	Platelet-Poor Plasma
PRP	Platelet-Rich Plasma
PT	Paraquat
qRT-PCR	Quantitative Reverse Transcription-Polymerase Chain Reaction

Abbreviation	Full Form
RESPA	Reversible Reference System Propagator Algorithms
RMSD	Root Mean Square Deviation
ROS	Reactive Oxygen Species
RT	Rotenone
SD	Standard Deviation
SV-NGF	Snake Venom Nerve Growth Factor
TIP3P	Three-Points Water Model
TNP	Trideca-Neuropeptide
TrkA	Tropomyosin Receptor Kinase A Receptor
UHPLC-MS/MS	Ultra-Performance Liquid Chromatography-Tandem Mass Spectrometer
PBS	Phosphate buffered saline
PPP	Platelet poor plasma
PRP	Platelet rich plasma
Q-RT PCR	Quantitative reverse transcription polymerase chain reaction
Q-TOF	Quadrapole time of flight
RCSB	Research collaborator for structural bioinformatics
RNA	Ribonuclic acid
ROS	Reactive oxygen species
RP-HPLC	Reversed-phase high-performance liquid chromatography
RP-UHPLC	Reversed-phase ultra-high-performance liquid chromatography
SGOT	Serum glutamic oxaloacetic transaminase
SGPT	Serum glutamic pyruvic transaminase
TBS	Tris-buffered saline
TCA	Trichloroacetic acid
TEMED	Tetramethylethylenediamine
TFA	Trifluoroacetic acid
WHO	World health organization
CNS	Central Nervous System
ALS	Amyotrophic Lateral Sclerosis
DALYs	Disability-Adjusted Life Years
A β	Amyloid-B

Abbreviation	Full Form
DAMP	Danger-Associated Molecular Pattern
IP3	Inositol 1,4,5-Triphosphate
PLC γ	Phospholipase C γ
JNK	C-Jun N-Terminal Kinase
YFP	Yellow Fluorescence Protein
miRNA	MicroRNAs
NTFs	Neurotrophic Factors
6-OHDA	6-Hydroxydopamine
MPP+	1-Methyl-4-Phenylpyridinium Iodide